CONVERSION OF GLUCOSE OVER SO_4^{2-}/ZRO_2-TIO_2 CATALYSTS IN AN EXTREMELY LOW ACID SYSTEM

Jun Zhang, Shubin Wu,* Hongdan Zhang, and Bo Li

SO_4^{2-}/ZrO_2-TiO_2 catalysts prepared by precipitation and impregnation methods were employed for glucose conversion. The basic structures of the prepared catalysts were characterized by XRD, BET, NH_3-TPD, XPS, and TEM techniques. The essential properties of SO_4^{2-}/ZrO_2 could be improved greatly by adding a suitable amount of TiO_2. High BET area and pore volume favored glucose conversion. The conversion rate of glucose into levulinic acid catalyzed by SO_4^{2-}/ZrO_2-TiO_2 increased significantly in an extremely low acid system, indicating that the acidic condition was favorable for levulinic acid formation. The combined yield of 5-hydroxymethylfurfural and levulinic acid reached 28.8% with the presence of SO_4^{2-}/ZrO_2-TiO_2 when the Zr-Ti molar ratio was 5:5 at 170 °C for 2 h in the extremely low acid system. Studies on catalyst recycling were also further investigated in this study.

Keywords: SO_4^{2-}/ZrO_2-TiO_2; 5-hydroxy methylfurfural; Levulinic acid; Extremely low acid system

*Contact information: State Key Laboratory of Pulp and Paper Engineering, South China University of Technology, Guangzhou, Guangdong, 510640, China; * Corresponding author: shubinwu@scut.edu.cn*

INTRODUCTION

Efficient production of commodity chemicals from renewable biomass has been one of the hottest topics in the field of energy and resources (Govindaswamy and Vane 2010; Zhao *et al.* 2007; Girisuta *et al.* 2006). As a class of green renewable energy resources, biomass has the advantages of being abundant, sustainable, and environmentally friendly. Glucose derived from biomass is an important feedstock for the production of green platform chemicals such as 5-hydroxymethyl-2-furaldehyde (HMF) and levulinic acid (LA) (Cen *et al.* 2003; French and Czernik 2010; Chum and Overend 2001). It has been widely accepted that HMF is a product of the facile, acid-catalyzed dehydration of carbohydrate, and levulinic acid can be obtained from a subsequent rehydration reaction of HMF (see Scheme 1). There are many studies on the conversion of carbohydrate into HMF and LA, but the major concern is that the conventional reaction system is acidic, and a relatively high reaction temperature is needed to increase final yield. The earliest research on HMF preparation suggested that the yield of HMF is much higher under acidic reaction conditions with D-fructose as raw material (Hales *et al.* 1963; Fitzpatick 1966). In addition, relevant studies showed that HMF yield could be improved greatly by adding organic solvents such as DMSO (Brown *et al.* 1982), n-butanol (Peniston 1956), or acetonitrile (Brown *et al.* 1982). With the progress of research, supercritical acetone/water binary system (Bicker *et al.* 2003), subcritical water (Asghari *et al.* 2006), and ionic liquid (Lansalot-Matras *et al.* 2003; Hu *et al.* 2008;

Moreau *et al.* 2006; Bao *et al.* 2008) were employed for the preparation of HMF from various materials.

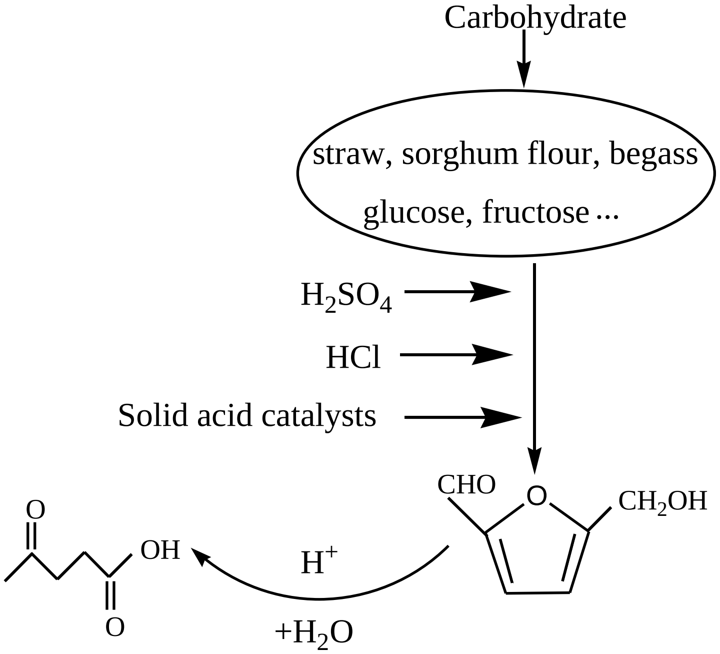

Scheme 1. Reaction network for the conversion of glucose into HMF and LA

As for the production of LA, previous studies showed that biomass resources including straw (Yan *et al.* 2008), sorghum flour (Fang and Hanna 2002), and bagasse (Rodriguez 1972) can be used as raw materials with HCl or H_2SO_4 as catalyst. However, the reaction condition was rigorous, *e.g.*, the reaction equipment should be corrosion-resistant, and the use of high concentration inorganic acid would lead to serious environmental pollution. To solve these problems, many efficient catalysts and reaction systems have been developed for the conversion of biomass resources. For example, Wei *et al.* (2004) reported that the niobic acid prepared by direct water-washing favored the formation of LA, and a LA yield of 9.5% was obtained with corresponding selectivity of 10.0%. Zeng and coworkers (2010) investigated the catalytic properties of a novel MFI-type zeolite with different SiO_2/Al_2O_3 ratio on the dehydration of glucose to LA in subcritical water and found that the strength of acidic sites and the pore of the zeolites had significant effects on LA formation. Moreover, the highest LA yield of 35.8 molar% was achieved at a reaction time of 8 h and a temperature of 180 ^{o}C. Their team also used Al-Zr mixed oxides for the conversion of glucose in hot compressed water, and the yields of LA and HMF were only 6.1 and 14.4 molar% (Zeng *et al.* 2009). Although the LA yield may be improved by using various modified catalysts, high yield still requires a low reactant concentration, a long reaction time, and a high inorganic acid concentration. Therefore it is not economical to scale up, and an efficient reaction system should be developed.

In this paper, SO_4^{2-}/ZrO_2-TiO_2 catalysts with different molar ratios of Zr to Ti were examined for glucose conversion in 0.01 wt.% H_2SO_4 solution. Sulfated solid acid catalysts had several merits, such as better acidity and easy separation. Also, the extremely low acid system was conducive to enhancing LA yield and is environmentally friendly. It also could decrease the loss of sulfur content in catalysts, which would prevent the rapid inactivation of SO_4^{2-}/ZrO_2-TiO_2. The specific relationship between catalyst properties and product formation was investigated. The total yield of HMF and LA also was investigated in this study due to the wide applications of these two compounds in the chemical industry. This research may provide a feasible route for industrial application of solid acid catalysts in glucose conversion. Studies on process optimization will be done in subsequent work.

EXPERIMENTAL

Materials

$TiCl_4$, $ZrOCl_2$•$8H_2O$, glucose, HMF, and LA were purchased from Shanghai Jingchun Reagent Co., Ltd. All of these chemicals used were of analytical grade.

Catalysts Preparation

SO_4^{2-}/ZrO_2-TiO_2 catalysts were prepared by precipitation and impregnation. The main preparation process of SO_4^{2-}/ZrO_2 is presented below. $ZrOCl_2$•$8H_2O$ was dissolved in deionized water to prepare a 0.4 molar/L zirconium ion containing solution. Concentrated ammonia was added to adjust the Zr solution to a pH value in the range 9 to 10. Then the solution was aged for 24 h to form $Zr(OH)_4$. The obtained precipitate was thoroughly washed with deionized water until chloride was rinsed out, based on $AgNO_3$ detection. The product was dried at 110 °C for 24 h. The dried precipitate was ground to below 60-mesh size, then impregnated in a 0.5 molar/L H_2SO_4 solution stirred at 500 rpm for 1 h. The precipitated solid was filtered, subsequently dried at 110 °C for 12 h, and finally calcined at 550 °C for 3 h to obtain SO_4^{2-}/ZrO_2. The SO_4^{2-}/TiO_2 was prepared with the same procedure with $TiCl_4$ as raw material instead of $ZrOCl_2$•$8H_2O$. For the preparation of SO_4^{2-}/ZrO_2-TiO_2 catalysts, co-precipitates of $Zr(OH)_4-Ti(OH)_4$ with different molar ratios of Zr to Ti were obtained by adding concentrated ammonia to a mixed aqueous solution of $ZrOCl_2$•$8H_2O$ and $TiCl_4$ with mixing until the pH reached 9 to 10. The following procedures were the same as in the preparation of SO_4^{2-}/ZrO_2.

Catalyst Characterization

X-ray powder diffraction (XRD) was performed in a Bruker D8 Advance diffractometer with Cu Kα radiation. The operating voltage and current were 40 kV and 40 mA, respectively. The step length was 0.02 degree with a scanning rate of $2°\cdot min^{-1}$. The morphology of the catalysts was analyzed with a transmission electron microscope (TEM) JEOL JEM-100CX operating at 100 kV. X-ray photoelectron spectroscopy (XPS) measurements were performed on a Kratos Ultra system employing an Al Kα radiation source. Samples were outgassed in a vacuum oven overnight before XPS measurements. The binding energies for each spectrum were calibrated with a C 1s spectrum of 284.6

eV. Survey spectra for each sample over a binding energy range of 0 to 1100 eV were recorded at a pass energy of 160 eV and resolution of 1 eV per step. High-resolution spectra of O 1s, S 2p, Ti 2p, and Zr 3d were recorded at a pass energy of 40 eV and resolution of 0.1 eV per step for quantitative measurements of binding energy and atomic concentration. The pore size and volume of $SO_4^{2-}/ZrO_2\text{-}TiO_2$ catalysts were determined following the standard nitrogen adsorption method using a Micromeritics Tristar 3020 instrument. Specific surface areas were calculated using the BET equation. Prior to analyses, all samples were degassed at 120 °C and 10^{-4} Torr pressure for 8 h to evacuate the physically adsorbed moisture.

The measurements of acidity of the samples were carried out in a Micromeritics AutoChemII 2920 chemisorption analyzer following an NH_3 temperature-programmed desorption (TPD) method. The sample was heated up to 600 °C at the rate of 15 °C/min and kept for 30 min in a flow of He gas (20 mL/min) to remove adsorbed species on the surface. Then the sample was cooled down to 100 °C in He flow, followed by adsorption of NH_3 in 10% NH_3 gas flow (balance He, 20 mL/min) for 1 h. After flushing with He for 1 h to remove physically adsorbed NH_3, the TPD data were measured from 100 °C to 600 °C with a ramp of 15 °C/min.

Catalytic Reaction

The conversion of glucose to HMF and LA was carried out in a high-pressure reactor (PARR 5500). Then 0.15 g solid acid catalysts, 1.5 g glucose, and 30 mL H_2O (0.01 wt.% H_2SO_4) were charged to the reactor. Next the reactor was sealed and purged with nitrogen gas. Subsequently the nitrogen gas was discharged from the reactor and the reaction was carried out at 170 °C for 2 h at a stirring rate of 600 rpm. After reaction, the obtained liquid phase samples were filtered and stored in the refrigerator before analysis. The used solid acid catalysts were dried and calcined at 550 °C for the next use.

An HPLC system (Agilent 1100) with C18 column and ultraviolet detector was employed to determine the concentration of HMF, using a 3:7 v/v methanol:water as the mobile phase at a flow rate of 1.0 mL/min with a column temperature of 25 °C. The glucose residue was analyzed by ion chromatography (Dionex ICS-3000) with a CarboPac^{TM} PA1 column. The eluents were NaOH and CH_3COONa with a flow rate of 0.25 mL/min. The sample loop had a volume of 50 μL. The column temperature was 30 °C. LA was analyzed by ion chromatography (Dionex ICS-3000) with IonPac^{R} AS11-HC column. The eluents were NaOH and water with a flow rate of 1.0 mL/min. Sample loop had a volume of 50 μL. The column temperature was 30 °C. Glucose conversion, yields of main products, and corresponding product selectivity (*i.e.*, HMF, LA and formic acid) were calculated as follows:

Glucose conversion (wt.%) = [(mass of starting glucose – mass of glucose after reaction) / mass of starting glucose] *100 %

Product yield (wt.%) = [mass of the product / mass of starting glucose] *100 %

Product selectivity (%) = [product yield / glucose conversion] *100 %.

RESULTS AND DISCUSSION

Catalyst Characterization

XRD test

Phase identification of the prepared catalysts was performed by XRD, as given in Fig. 1. For SO_4^{2-}/TiO_2, several peaks appeared at 2θ = 25.3°, 37.9°, 47.9°, 54.3°, and 62.6°, which indicated the formation of an anatase phase. In the case of SO_4^{2-}/ZrO_2, it comprised a mixture of tetragonal and cubic phases as identified by the presence of peaks at 2θ = 30.1°, 35.3°, and 2θ = 50.2°, 60.2°, respectively, and the main phase was tetragonal. The XRD patterns of SO_4^{2-}/ZrO_2-TiO_2 with different Zr/Ti molar ratios were quite different from that of a single compound. Two broad peaks located at 2θ = 30.2° and 2θ = 35.2° were found on the patterns of 9Zr-Ti, which represented the tetragonal phase of ZrO_2. Other broad peaks from 40° to 80° could also be observed in the samples, which indicated a strong interaction between the two components and the formation of the Ti-O-Zr solid suspension. The SO_4^{2-}/ZrO_2-TiO_2 (Zr-9Ti) catalyst with a high concentration of TiO_2 had peaks similar to pure SO_4^{2-}/ TiO_2, but the intensity of the related peaks (2θ = 25.3°, 37.9°, 47.9°, and 54.3°) decreased with decreasing titanium concentration, and the characteristic peaks of SO_4^{2-}/ZrO_2 were hard to detect. Catalysts SO_4^{2-}/ZrO_2-TiO_2 with molar ratio of Zr-Ti at 7:3, 5:5, and 3:7 were amorphous, as seen from the XRD patterns. This was probably due to the presence of ZrO_2 in the samples, which could effectively suppress the growth of crystallites (Fu *et al.* 1996; Wang, *et al.* 2006). Meanwhile, the calcination temperature may not be suitable for the crystallization of these catalysts, and the optimum crystallization temperature changed with correspond-ding catalyst components. However, the results obtained in the catalytic experiment demonstrated that the specific product yields were not affected by the crystallinity of these catalysts.

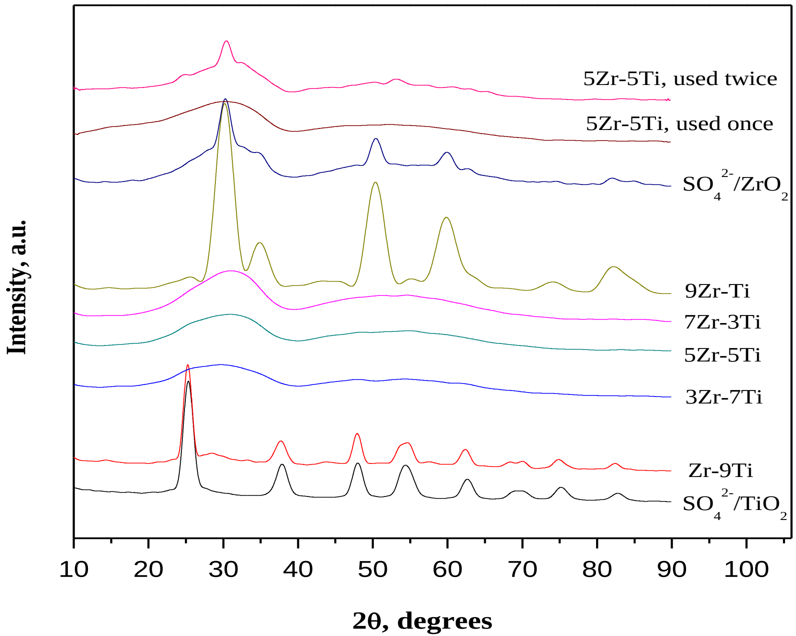

Fig. 1. Powder XRD patterns of SO_4^{2-}/ZrO_2-TiO_2 catalysts with different Zr/Ti molar ratios

For the recycled SO_4^{2-}/ZrO_2-TiO_2 (5Zr-5Ti), there were no obvious changes in the crystalline phase after being used twice. But it was noted that there was a spike at $2\theta = 30.2°$ when the catalyst was used for the second time. The main reason could be that the used catalysts were calcined at 550 ^oC after each use, so the specific crystalline phase may be apparent after calcining for the second time.

Textural properties of SO_4^{2-}/ZrO_2-TiO_2 catalysts

The textural properties of SO_4^{2-}/ZrO_2-TiO_2 catalysts are given in Table 1. It can be seen that the BET area and pore volume of SO_4^{2-}/ZrO_2 catalysts were improved when adding TiO_2, and the surface area reached its highest level at a Zr-Ti molar ratio of 3:7. Then the BET area and pore volume decreased slowly with further addition of ZrO_2. It is well known that high pore volume favors the whole reaction, because it could facilitate mass exchange between reactants and catalysts. It is notable that BET area and pore volume of SO_4^{2-}/TiO_2 were significantly higher than those of SO_4^{2-}/ZrO_2. This may be determined by their intrinsic properties and processing methods. All of these illustrated that properly increasing TiO_2 content could improve the surface properties of SO_4^{2-}/ZrO_2 due to the combination and interaction among Zr, O, and Ti atoms.

Table 1. Textural Properties of SO_4^{2-}/ZrO_2-TiO_2

Samples	SO_4^{2-}/ZrO_2	9Zr-Ti	7Zr-3Ti	5Zr-5Ti	3Zr-7Ti	Zr-9Ti	SO_4^{2-}/TiO_2
BET area (m^2/g)	29.9	56.3	131.0	151.9	160.7	53.1	97.0
Pore volume (cm^3/g)	0.036	0.09	0.19	0.25	0.30	0.15	0.13
Pore size (nm)	6.7	8.1	6.9	6.9	8.3	11.1	5.3

NH_3-TPD measurement

The acidic properties and catalytic activity of sulphated oxides/mixed oxides are dependent on sulfate groups and their intrinsic properties. The NH_3-TPD profiles of the prepared catalysts with different Zr/Ti molar ratios are shown in Fig. 2. NH_3 molecules can be adsorbed on the acid sites of catalysts and be removed during the heating process. Acid sites of SO_4^{2-}/ZrO_2-TiO_2 catalysts were distributed in two desorption regions at about 100 to 200 ^oC and 500 to 600 ^oC. Temperatures of NH_3 desorption peaks and the quantities of total acid sites are summarized in Table 2. It was found that first the total acidity of these catalysts increased and then decreased with the addition of TiO_2. The maximum total acidity was obtained at a Zr/Ti molar ratio of 7:3. The amount of strong acid sites generally rose when decreasing the Zr/Ti molar ratio. It has been reported that high surface acidity of TiO_2-ZrO_2 binary oxide contributes to the charge imbalance because of the generation of Ti-O-Zr bonding (Wu *et al.* 1984). Furthermore, the acidity of SO_4^{2-}/TiO_2 was higher than SO_4^{2-}/ZrO_2. This may be due to the better impregnation effect of TiO_2 in 0.5 molar/L H_2SO_4 solution. Also TiO_2 could integrate well with SO_4^{2-} after being calcined at 550 ^oC. It was reported that LA formation was related to the amount of strong acid sites, but the experimental results were not consistent with the numbers in the literature (Asghari and Yoshida 2006). It is possible that both the quantities of total acid sites and the acidic reaction system affected the conversion. The quantities of acid sites of these catalysts probably related to the preparation processes such as impregnation in 0.5 molar/L H_2SO_4 solution or calcination at high temperature. As for NH_3-TPD measurement of recycled SO_4^{2-}/ZrO_2-TiO_2 (5Zr-5Ti) catalyst, it can be seen from Table 2 and Fig. 2 that the acidity of used catalysts decreased obviously including total and strong sites, and the temperature of strong sites also declined with the recycling of catalysts. It is worth noting that the amount of strong sites in the catalyst decreased significantly after using twice compared to weak sites.

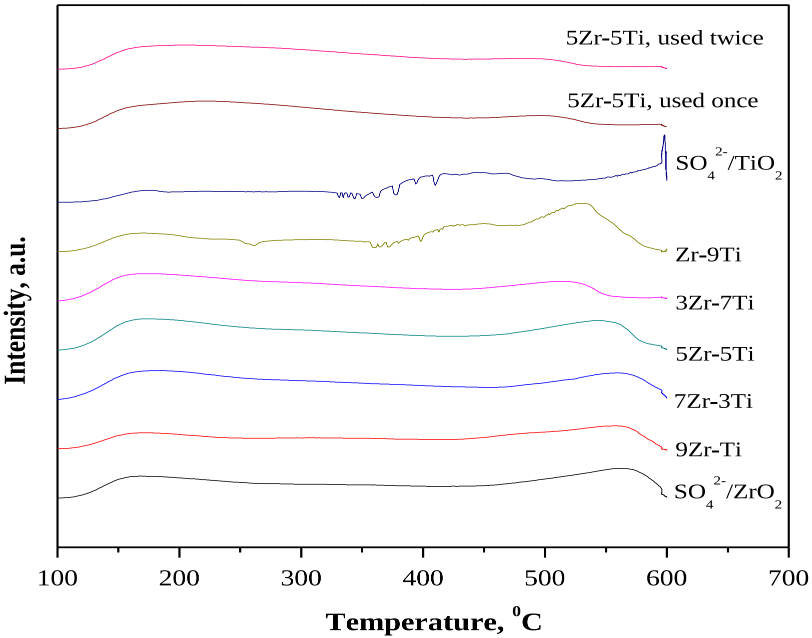

Fig. 2. NH_3-TPD profiles of SO_4^{2-}/ZrO_2-TiO_2 with different Zr/Ti molar ratios

Table 2. Acidity of SO_4^{2-}/ZrO_2-TiO_2 Catalysts Measured by NH_3-TPD

Samples	NH_3 desorption peaks (°C)	Amounts of acid sites (mmol/g)		
		Total	Weak sites	Strong sites
SO_4^{2-}/ZrO_2	165, 549	0.26	0.13	0.13
9Zr-Ti	173, 557	0.34	0.18	0.16
7Zr-3Ti	184, 560	0.53	0.35	0.18
5Zr-5Ti	173, 541	0.52	0.31	0.21
3Zr-7Ti	172, 516	0.51	0.29	0.22
Zr-9Ti	169, 529	0.48	0.16	0.32
SO_4^{2-}/TiO_2	356, 525	0.45	0.20	0.25
5Zr-5Ti-once	221, 493	0.46	0.36	0.10
5Zr-5Ti-twice	207, 481	0.27	0.21	0.06

TEM study

Figure 3 shows transmission electron microscope (TEM) images at high magnification, revealing the structure of SO_4^{2-}/ZrO_2-TiO_2 catalyst. As seen from parts (c), (d), and (e), the crystallinity of corresponding catalysts was relatively low. There were only little crystals, and a partially amorphous state was observed, which was in line with the results indicated in Fig. 1. The crystallization of SO_4^{2-}/ZrO_2 also was not satisfactory. The major reason was that the calcination temperature of this catalyst may not have been optimal, resulting in low crystallinity. The added ZrO_2 acted as a crystal growth inhibitor, leading to the formation of smaller grain size compared to SO_4^{2-}/TiO_2. For SO_4^{2-}/TiO_2

catalysts and SO_4^{2-}/ZrO_2-TiO_2 (Zr-9Ti) catalysts, crystal particles with particle diameters in the nanometer range appeared to form; in addition, the particles were of regular shape, good dispersivity, and uniform particle size. The TEM images clearly show how ZrO_2 controlled the particle size and shape of TiO_2.

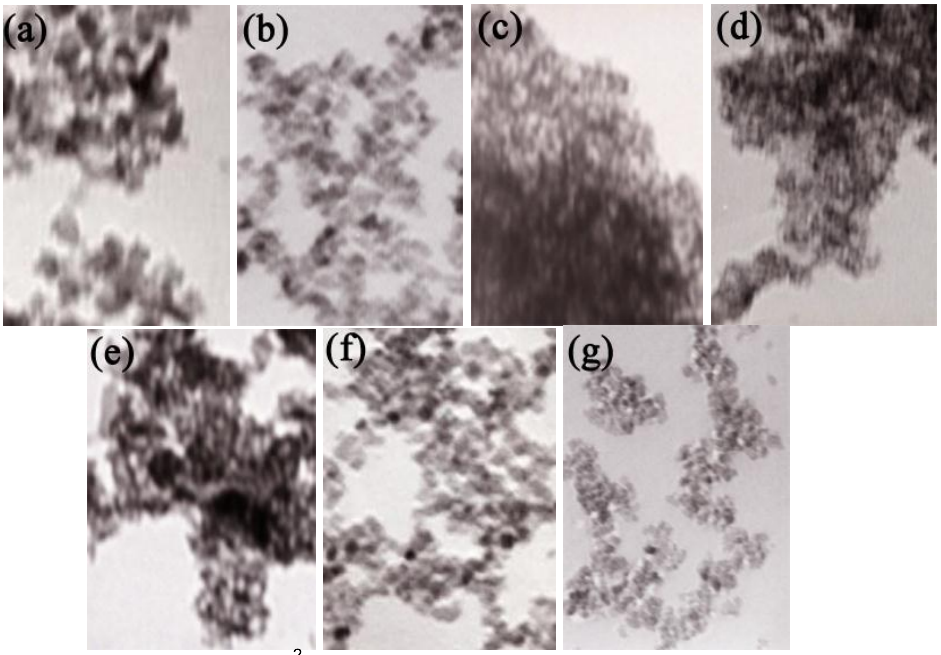

Fig. 3. TEM images of catalysts SO_4^{2-}/ZrO_2-TiO_2 with different molar ratios of Zr to Ti: (a) SO_4^{2-}/ZrO_2, 150,000X; (b) 9Zr-Ti, 150,000X; (c) 7Zr-3Ti, 100,000X; (d) 5Zr-5Ti, 100,000X; (e) 3Zr-7Ti, 100,000X; (f) Zr-9Ti, 150,000X; (g) SO_4^{2-}/TiO_2, 150,000X

XPS Analysis

The main reason for conducting XPS analysis was to obtain information regarding the chemical environment and elemental concentrations presented in catalysts SO_4^{2-}/ZrO_2-TiO_2. Table 3 lists the elemental compositions as confirmed by the XPS spectral analysis. A small amount of S was detected in all samples. It is important to note that the product yield was not significantly affected by sulfur content. High-resolution scans of the XPS spectra of S 2p, Ti 2p, Zr 3d, and O 1s with different intensity scale as ordinate are shown in Fig. 4. The binding energy of the Zr 3d photoelectron peaks was observed at 181 eV for the Zr $3d_{5/2}$ line and 183 eV for the Zr $3d_{3/2}$ line. However, the binding energy of the Zr $3d_{5/2}$ line in pure ZrO_2 sample ranges from 182.2 to 182.5 eV (Reddy 2002). A decrease in the binding energy of Zr 3d line for SO_4^{2-}/ZrO_2 and 7Zr-3Ti was probably caused by the formation of $ZrTiO_4$. A similar phenomenon was also observed in the SO_4^{2-}/TiO_2 sample. The binding energy of the Ti $2p_{3/2}$ in pure TiO_2 sample was 458.5 eV, but it decreased to 457.1 eV, and high binding energy of Ti $2p_{1/2}$ in 463.8 eV was found in the catalysts. The O 1s photoelectron spectrum was much more complicated due to the overlapping contributions of oxygen from zirconia, titanium, and sulfate. It can be noted from Fig. 4 that a wide range of the O 1s peak was detected. The S was on the surface of catalysts, and a distinct S $2p_{3/2}$ photoelectron peak was observed at about 168.0 eV, ascribable to the sulfate. For recycled SO_4^{2-}/ZrO_2-TiO_2 (5Zr-5Ti) catalyst, it can be seen from Table 3 that the sulfur in catalyst was being lost, which decreased from 5.1 to 3.0% after the second use. This may lead to a significant decrease in corresponding catalyst acidity. The binding energies of each element remained largely unchanged, as shown in Fig. 5.

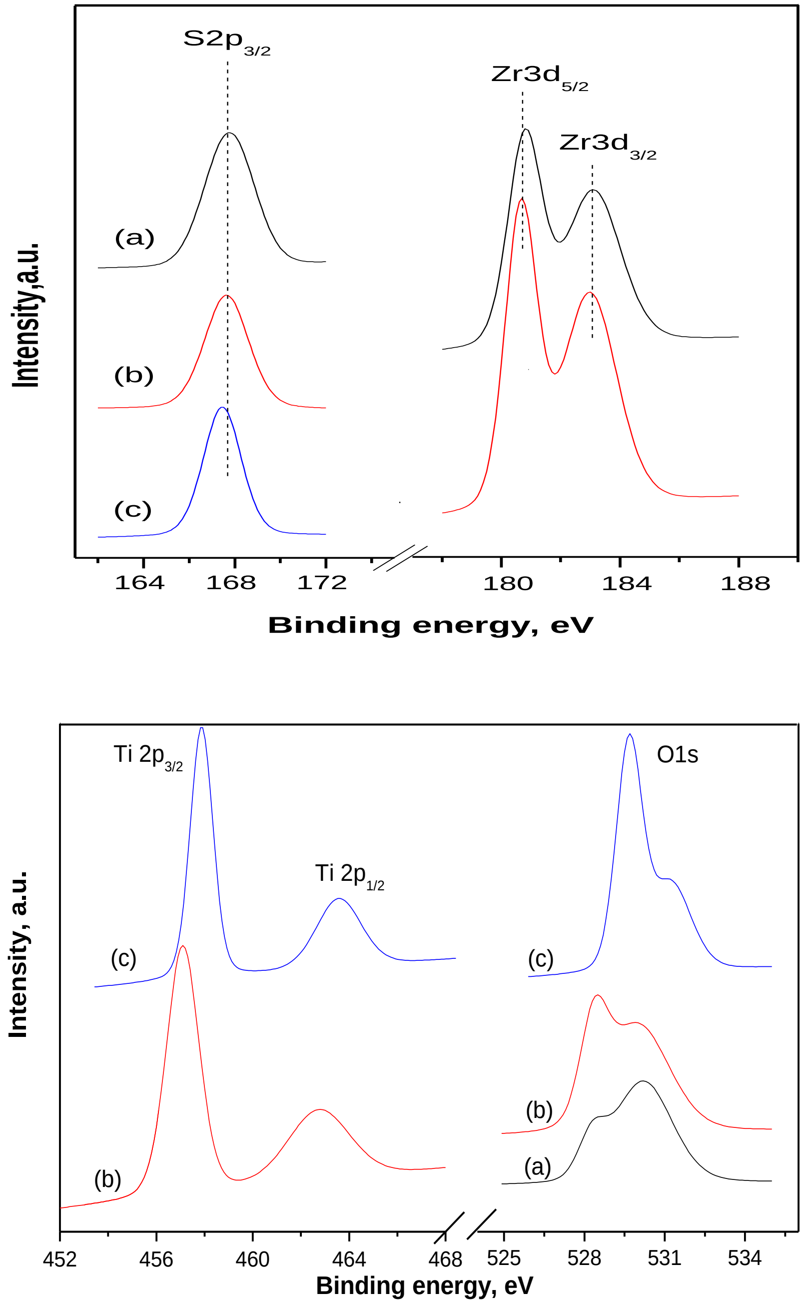

Fig. 4. XPS spectra of S 2p, Zr 3d, Ti 2p and O 1s of SO_4^{2-}/ZrO_2-TiO_2 catalysts, (a) SO_4^{2-}/ZrO_2, (b) SO_4^{2-}/ZrO_2-TiO_2 (7Zr-3Ti), (c) SO_4^{2-}/TiO_2. The intensity scales of S 2p, Ti 2p, Zr 3d, and O 1s spectra were different

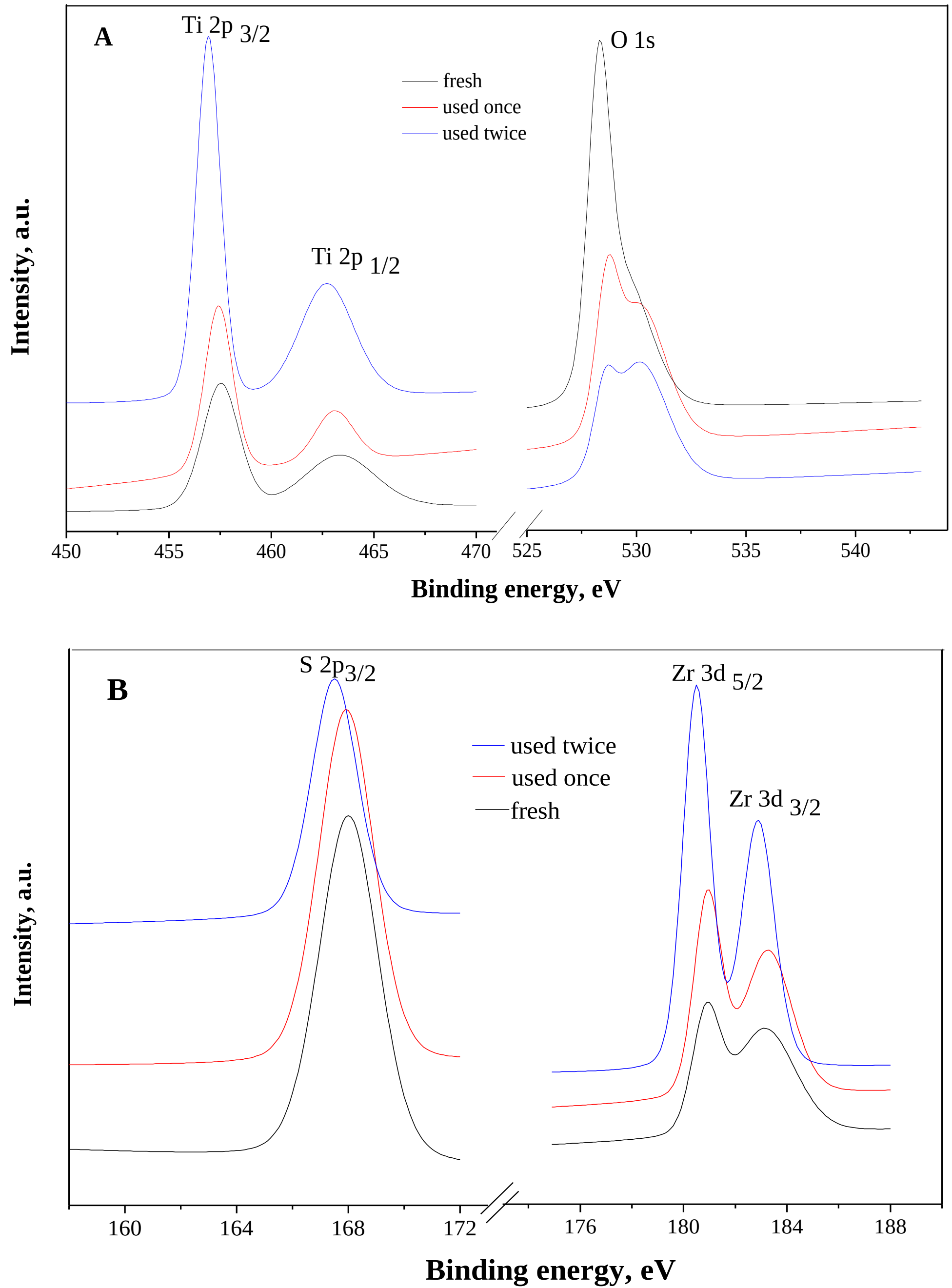

Fig. 5. XPS spectra of S 2p, Zr 3d, Ti 2p and O 1s of fresh and used SO_4^{2-}/ZrO_2-TiO_2 (5Zr-5Ti) catalysts. The intensity scales of S 2p, Ti 2p, Zr 3d, and O 1s spectra were different

Catalytic Conversions of Glucose over SO_4^{2-}/ZrO_2-TiO_2 Catalysts

Table 4 shows the effect of different reaction conditions on the yield of HMF, LA, and formic acid (FA). When the reaction was carried out in 0.01 wt.% H_2SO_4, the LA yield was very low, with HMF as the main product. This was because the acidity of 0.01 wt.% H_2SO_4 was limited and little HMF was available to be further converted into LA. The product was mainly HMF with SO_4^{2-}/ZrO_2 as catalyst in aqueous solution, and the LA yield was still lower. Then dehydration of glucose with SO_4^{2-}/ZrO_2 catalyst was carried out in 0.01 wt.% H_2SO_4. The LA yield increased significantly by 62.8% compared with SO_4^{2-}/ZrO_2 (H_2O) catalyst, and the HMF yield declined, since much HMF produced in this reaction condition was further converted to LA with increased system acidity. The results indicated that using 0.01 wt.% H_2SO_4 as a new catalytic system favored LA formation, and it also was friendly to the environment and helpful to the improvement of LA yield. Besides, the FA yield increased greatly with an increase in the acidity of the reaction system.

Table 3. Experimental Elemental Compositions by XPS Analysis for SO_4^{2-}/ZrO_2-TiO_2 Catalysts

Catalyst	S (%)	Zr (%)	Ti (%)	O (%)
SO_4^{2-}/ZrO_2	5.0	12.5	0	46.6
7Zr-3Ti	3.7	14.8	5.0	52.4
SO_4^{2-}/TiO_2	3.5	0	22.0	57.6
5Zr-5Ti-fresh	5.1	9.9	9.1	55.4
5Zr-5Ti-once	4.2	9.6	8.4	51.5
5Zr-5Ti-twice	3.0	11.9	10.4	52.0

Table 4. Comparison of the Catalytic Effect Under Different Reaction Conditions

Catalyst	HMF yield, %	LA yield, %	FA yield, %
[a] 0.01 wt.% H_2SO_4	5.9	0.3	0.4
[b] SO_4^{2-}/ZrO_2 (H_2O)	7.0	1.8	0.7
[c] SO_4^{2-}/ZrO_2 (0.01 wt.% H_2SO_4)	5.0	2.9	0.9

Reaction conditions: glucose 1.5 g, 600 rpm, 170 °C, 2 h, (a) 30 mL 0.01 wt.% H_2SO_4; (b) SO_4^{2-}/ZrO_2 0.15 g, 30 mL H_2O; (c) SO_4^{2-}/ZrO_2 0.15 g, 30 mL 0.01 wt.% H_2SO_4

The effect of SO_4^{2-}/ZrO_2-TiO_2 with different Zr/Ti molar ratios on the conversion of glucose is shown in Table 5. The total (LA and HMF) yield also was taken into consideration in this study. First, the LA yield increased greatly with the reduction of Zr/Ti molar ratio, which reached the highest level of 18.4% at a Zr-Ti molar ratio of 5:5. As the Zr/Ti molar ratio decreased, the yield and selectivity of LA began to decline. And more notably, the amount of total sites in SO_4^{2-}/ZrO_2-TiO_2 catalysts exhibited the similar trend. However, no direct relationship between LA yield and the amount of strong acid sites was observed. It is worth noting that the LA yield or selectivity was higher when catalyzed by SO_4^{2-}/TiO_2 compared to SO_4^{2-}/ZrO_2, which may be related to the properties of corresponding catalyst such as acidity and BET area. Hence, the optimal catalyst for LA production was SO_4^{2-}/ZrO_2-TiO_2 at Zr/Ti molar ratio of 5:5. The total yield increased quickly as the molar ratio of Zr to Ti decreased. The highest yield of 28.8% was achieved at a Zr/Ti molar ratio of 5:5. Meanwhile, the total selectivity reached the maximum value at a Zr-Ti molar ratio of 7:3, which showed the same trend as LA selectivity. It was found that the total yield was higher when the reaction was catalyzed by SO_4^{2-}/TiO_2 compared to SO_4^{2-}/ZrO_2, which further demonstrated that SO_4^{2-}/TiO_2 is a better catalyst with high catalytic activity. It is well known that one mole of LA and one mole of FA are obtained per mole of HMF or glucose. It can be observed from Table 5 that when the Zr-Ti molar ratio decreased to 3:7, there was a great increase in FA yield. Then it began to decrease with a further increase in TiO_2 content. The main reason was that the total amount of acid sites were reduced, which may prevent the rapid degradation of HMF into LA and FA.

The same situation appeared in FA yield when catalyzed by SO_4^{2-}/TiO_2 compared to SO_4^{2-}/ZrO_2.

Table 5. The Yield and the Selectivity to Each Considered Product (HMF, LA, and FA)

Samples	SO_4^{2-}/ZrO_2	9Zr-Ti	7Zr-3Ti	5Zr-5Ti	3Zr-7Ti	Zr-9Ti	SO_4^{2-}/TiO_2
LA yield, %	2.9	3.9	14.3	18.4	13.5	10.6	8.4
LA selectivity, %	7.4	9.5	29.7	28.1	19.9	15.2	12.9
HMF yield, %	5.0	6.6	9.7	10.4	7.9	8.5	9.5
HMF selectivity, %	12.5	16.4	20.1	16.0	11.6	12.2	14.5
Total yield, %	7.9	10.5	24.0	28.8	21.4	19.1	17.9
Total selectivity, %	19.9	25.9	49.8	44.1	31.5	27.4	27.4
FA yield, %	0.9	1.9	2.8	2.9	4.5	1.8	1.4

Reaction conditions: solid acid catalysts 0.15 g, glucose 1.5 g, 30 mL 0.01 wt.% H_2SO_4, 600 rpm, 170 °C, 2 h

Because of the better catalytic activity of SO_4^{2-}/ZrO_2-TiO_2 (5Zr-5Ti) catalyst, it was recycled after each experiment by filtering the final solution and washing with de-ionized water. Then it was dried at 110 °C and calcined at 550 °C without other complex processing before the next use. As shown in Table 6, the catalytic activity decreased after being reused once, and the LA yield decreased from 18.4% to 12.9%. One possible reason that the catalyst acidity decreased significantly was the loss of sulfur. However, after recycling the catalyst twice, the total yield was not found to be reduced significantly. This result showed that although the catalyst acidity decreased sharply by recycling twice, much glucose also could be converted into HMF and partly transformed into LA. Through the recycling of catalysts, it was inferred that the acidity of used solid acid catalysts would be recovered by impregnation with diluted H_2SO_4 solution, then the corresponding catalytic activity could be enhanced.

Table 6. Effect of Recycling Time of Catalyst (5Zr-5Ti) on the Conversion of Glucose

Catalyst	fresh	used once	used twice
LA yield, %	18.4	12.9	10.0
Total yield, %	28.8	20.9	19.8
Total selectivity, %	44.1	43.2	41.3

Reaction conditions: fresh and used catalysts (5Zr-5Ti) 0.15 g, glucose 1.5 g, 30 mL 0.01 wt.% H_2SO_4, 600 rpm, 170 °C, 2 h

CONCLUSIONS

1. A series of catalysts, SO_4^{2-}/ZrO_2-TiO_2 catalysts with different molar ratios of Zr to Ti prepared by precipitation and impregnation were applied to catalyze glucose dehydration in an acid system at extremely low concentration.

2. The LA yield could be improved markedly with SO_4^{2-}/ZrO_2-TiO_2 as catalyst when the reaction was conducted under acidic conditions. LA formation was independent of the amount of strong acid sites in the solid acid catalysts.
3. BET analysis illustrated that a suitable increase of TiO_2 content could improve the surface properties of SO_4^{2-}/ZrO_2. Catalysts characterization of XRD and TEM suggested that the crystallinity of catalysts were not high.
4. The total yield reached 28.8% at 170 °C for 2 h while catalyzed by SO_4^{2-}/ZrO_2-TiO_2 with Zr-Ti molar ratio at 5:5 in 0.01 wt.% H_2SO_4.
5. Studies on catalyst recycling indicated that the catalytic activity of SO_4^{2-}/ZrO_2-TiO_2 catalysts still needed to be enhanced.

ACKNOWLEDGMENTS

This work was supported by the National High Technology Research and Development Program of China (863 Program), the Science and Technology Department of Guangdong Province, China (No. 2010y1-C071), the National Natural Science Foundation of China (No. 21176095), and the Major Research Projects of Guangdong Province, China (No. 2011A090200006).

REFERENCES CITED

Asghari, F. S., and Yoshida, H. (2006). “Dehydration of fructose to 5-hydroxymethylfurfural in sub-critical water over heterogeneous zirconium phosphate catalysts,” *Carbohydr. Res.* 314(16), 2379-2387.

Asghari, F. S., and Yoshida, H. (2006). “Acid-catalyzed production of 5-hydroxymethylfurfural from D-fructose in subcritical water,” *Ind. Eng. Chem. Res.* 45(7), 2163-2173.

Bao, Q. X., Qiao, K., and Tomida, D. (2008). “Preparation of 5-hydroxymethylfurfural by dehydration of fructose in the presence of acidic ionic liquid,” *Catal. Commun.* 9(6), 1383-1388.

Bicker, M., Hirth, J., and Vogel, H. (2003). “Dehydration of fructose to 5-hydroxymethylfurfural in sub- and supercritical acetone,” *Green Chem.* 5(2), 280-284.

Brown, D. W., Floyd, A. J., Kinsman, R. G., and Roshanhyphen, Y. (1982). “Dehydration reactions of fructose in non-aqueous media,” *J. Chem. Tech. Biotechnol.* 32(7-12), 920-924.

Cen, P. L., Mu, J. H., Zhao, C. H., and Lin, J. P. (2003).“Research and development on levulinic acid-a new-type green platform chemical from renewable resources,” *Chin. J. Bioprocess Eng.* 1(1), 17-23.

Chum, H. L., and Overend, R. P. (2001). “Biomass and renewable fuels,” *Fuel Process. Technol*. 71(1-3) 187-195.

Fang, Q., and Hanna, M. A. (2002). "Experimental studies for levulinic acid production from whole kernel grain sorghum," *Bioresour. Technol*. 81(3), 187-192.

Fitzpatrick, H. D. (1966) "Process for carrying out reactions involving sugars and their derivatives with reagents therefore," GB 1019512.

French, R., and S. Czernik. (2010). "Catalytic pyrolysis of biomass for biofuels production," *Fuel Process. Technol.* 91(1), 25-32.

Fu, X., Clark, L. A., Yang Q., and Anderson, M. A. (1996). "The enhanced photocatalytic performance of titania-based binary metal oxides: $Ti0_2$/$Si0_2$/$Zr0_2$," *Environ. Sci. Technol.* 30(2), 647-653.

Girisuta, B., Janssen, L. P. B. M., and Heeres, H. J. (2006). "Green chemicals: A kinetic study on the conversion of glucose to levulinic acid," *Chem. Eng. Res. Des*. 84(5), 339-349.

Govindaswamy, S. and Vane, L. M. (2010). "Multi-stage continuous culture fermentation of glucose-xylose mixtures to fuel ethanol using genetically engineered saccharomyces cerevisiae 424A," *Bioresour. Technol.* 101(4), 1277-1284.

Hales, R. A., Le Maistre, J. W., and Orth Jr., G. O. (1963). "Preparation of hydroxy-methyl furfural," *U.S. Patent* 3071599.

Hu, S. Q., Zhang, Z. F., and Zhou, Y. X. (2008). "Conversion of fructose to 5-hydroxy-methylfurfural using ionic liquids prepared from renewable materials," *Green Chem.* 10(12), 1280-1283.

Lansalot-Matras, C. and Moreau, C. (2003). "Dehydration of fructose into 5-hydroxy-methylfurfural in the presence of ionic liquids," *Catal. Commun.* 4(10), 517-520.

Li, C. Z., Zhang, Z. H., and Zhao, Z. B. K. (2009). "Direct conversion of glucose and cellulose to 5-hydroxymethylfurfural in ionic liquid under microwave irradiation," *Tetrahedron Lett.* 50(38), 5403-5405.

Moreau, C., Finiels, A., and Vanoye, L. (2006). "Dehydration of fructose and sucrose into 5-hydroxymethylfurfural in the presence of 1-H-3-methyl imidazolium chloride acting both as solvent and catalyst," *J. Molar. Catal. A: Chemical* 253(1-2), 165-169.

Peniston, Q. P. (1956). Manufacture of 5-hydroxymethyl-2-furfural: *U.S. Patent* 2750394.

Reddy, B. M., Sreekanth, P. M., Yamada, Y., Xu, Q., and Kobayashi, T. (2002). "Surface characterization of sulfate, molarybdate, and tungstate promoted TiO2-ZrO2 solid acid catalysts by XPS and other techniques," *Appl. Catal. A: Gen.* 228(1-2), 269-278.

Rodriguez, R. E. (1972). "Process for jointly producing furfural and levulinic acid from bagasse and other lignocellulosic material," *U.S. Patent* 3701789.

Wei, C. L., Chen, F. Q., Zhang, H. H., and Zhan X. L. (2004). "Hydrolysis of glucose solutions over niobic acid as solid acid catalyst," *Industrial Catal*ysis 12(12), 46-49.

Wu, J. C., Chung, C. S., Ay, C. L., and Wang, I. (1984). "Nonoxidative dehydrogenation of ethylbenzene over TiO_2---ZrO_2 catalysts: II. The effect of pretreatment on surface properties and catalytic activities," *J. Catal.* 87(1), 98-107.

Wang, X., Yu, J. C., Chen, Y., Wu, L., and Fu, X. (2006). "ZrO_2-modified mesoporous nanocrystalline $TiO_{2-x}N_x$ as efficient visible light photocatalysts," *Environ. Sci. Technol.* 40(7), 2369-2374.

Yan, L. F., Yang, N. K., and Pang, H. L. B. (2008). "Production of levulinic acid from bagasse and paddy straw by liquefaction in the presence of hydrochloride acid," *Clean-Soil, Air, Water* 36(2), 158-163.
Zeng, W., Cheng, D. G., Chen, F. Q., and Zhan, X. L. (2009). "Catalytic conversion of glucose on Al–Zr mixed oxides in hot compressed water," *Catal. Lett.* 133(1-2), 221-226.
Zeng, W., Cheng, D. G., Zhang, H. H., Chen, Q. F., and Zhan, X. L. (2010). "Dehydration of glucose to levulinic acid over MFI-type zeolite in subcritical water at moderate conditions," *Reac. Kinet. Mech. Cat.* 100(2), 377-384.
Zhao, H. B., Holladay, J. E., Brown, H., and Zhang, Z. C. (2007). "Metal chlorides in ionic liquid solvents convert sugars to 5-hydroxymethylfurfural," *Science* 316(5831), 1597-1600.

Article submitted: February 17, 2012; Peer review completed: May 28, 2012; Revised version received and accepted: July 9, 2012; Published: July 11, 2012.